

# Optoelectronic properties of zinc oxide: A first-principles investigation using the Tran-Blaha modified Becke-Johnson potential

R. M. V. S. Almeida and J. S. de Almeida\*

*Instituto de Física, Universidade Federal da Bahia,*

*Campus Universitario de Ondina, 40210-340 Salvador, Bahia, Brazil*

A. L. da Rosa

*Instituto de Física, Universidade Federal de Goiás, 74.690-900 Goiânia, Goiás, Brazil*

(Dated: March 22, 2021)

## Abstract

In this work we use density functional theory (DFT) to investigate the influence of semi-local exchange and correlation effects on the electronic and optical properties of zinc oxide. We find that the inclusion of such effects using the Tran-Blaha modified Becke-Johnson potential yields an excellent description of the electronic structure of this material giving energy band gap which is systematically larger than the one obtained with standard local functionals such as the generalized gradient approximation. The discrepancy between the experimental and theoretical band gaps is then significantly reduced at a computational low cost. We also calculated the dielectric functions of ZnO and find a violet shift to the absorption edge which is in good agreement with experimental results.

---

\* jailton\_almeida@hotmail.com

## I. INTRODUCTION

Zinc oxide (ZnO) is a wide band gap semiconductor with promising application in laser diodes, light emitting diodes, transparent electrodes and gas sensors [1]. Although there has been a great progress in samples fabrication, controlling the conductivity in ZnO is still a challenge due to the presence of impurities and defects [2, 3]. From the theoretical side, the correct description of the band gap is of paramount importance for the understanding of impurity and defect states in semiconductors. It is a common understanding that the use of local exchange-correlation functionals wrongly describe the ZnO band gap. This can also lead to misleading conclusions on the location of the impurity and defect states [3–7]. The experimental band gap of ZnO is 3.4 eV [8] while the calculated value using GGA-PBE [9] yield 0.7-0.9 eV [4–6]. There are different schemes available to improve the band gap, one of the most common being hybrid functionals [10, 11]. More sophisticated approaches, such as the GW method [12–14] has become the state of the art but it is still computationally cost. It has been shown that partially or fully self-consistent schemes [3, 15–19], in which either Green’s function  $G$  or both the Green’s function and the dielectric matrix are updated can improve the agreement with experiments. Although for small cells the calculations are feasible when treating larger systems required to investigate defects these schemes are computationally much more demanding compared to LDA or GGA and for many systems the GW approximation is still prohibitive. Therefore one looks always for alternative methods which are computationally at similar costs as local/semi-local DFT calculations and at the same time could improve band gaps and description of energy level positions.

Recently proposed Tran-Blaha modified version of the Becke-Johnson potential (TB-mBJ) [20] has proved to be a successful method for accurate band gaps of semiconductors and insulators [21–25]. Furthermore, it has a computational cost as the LDA or GGA. For ZnO, it has been shown to lead to band gaps close to the experimental values [8, 24, 25].

In this work, we use the Tran-Blaha modified Becke-Johnson (TB-mBJ) potential [20] to investigate the electronic structure and optical response of ZnO. We found that TB-mBJ potential greatly improves the description of the electronic structure of ZnO compared to GGA, but still has several drawbacks with respect to GW calculations.

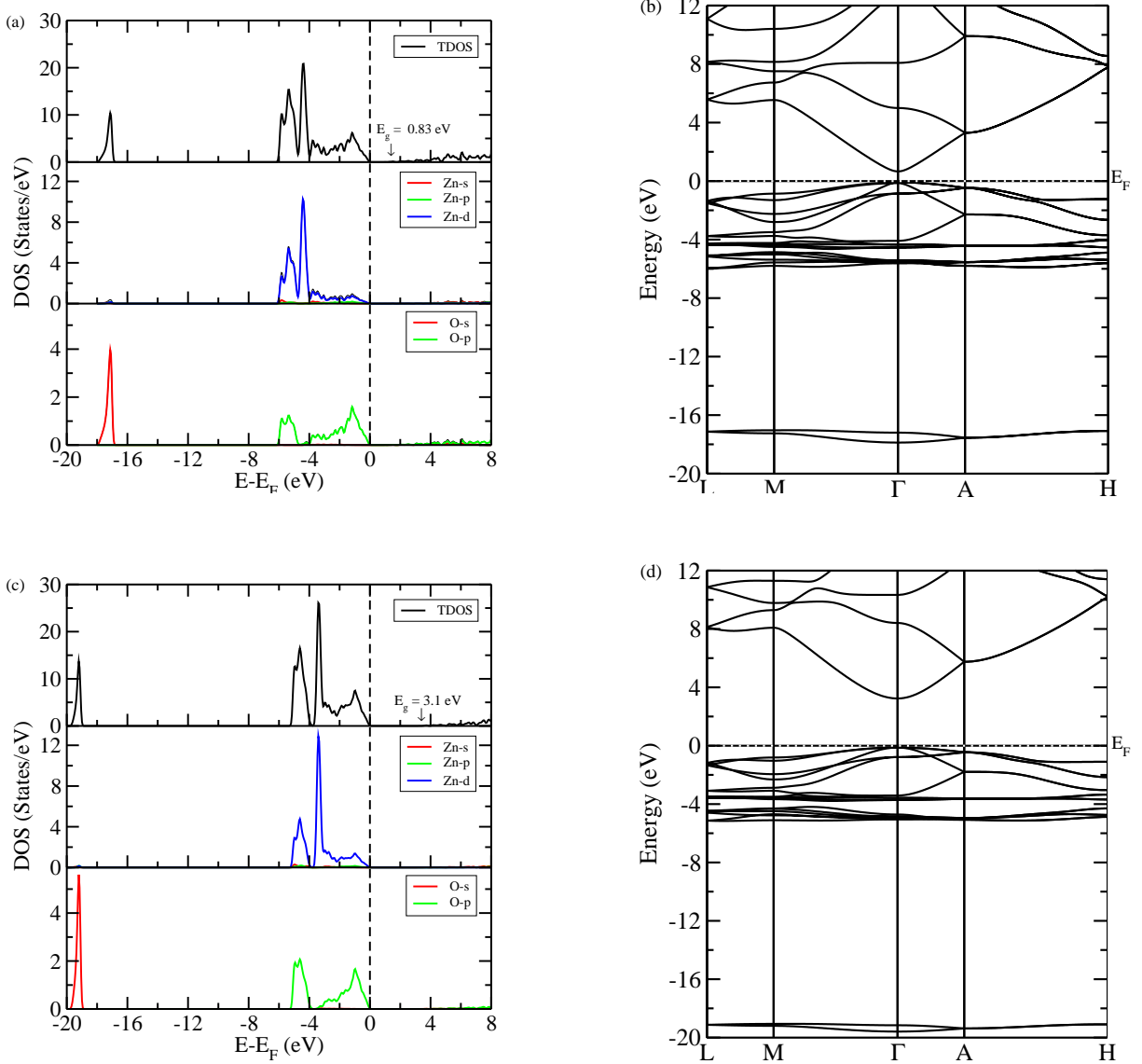


FIG. 1. Total and partial density of states (DOS) (a) and band structure (b) of ZnO with GGA-PBE functional (upper panel). Total and partial DOS (c) and band structure (d) of ZnO using TB-mBJ potential (lower panel).

## II. COMPUTATIONAL DETAILS

To investigate the optoelectronic properties of ZnO, we have used density-functional theory within the projected augmented wave (PAW) method [26] and the GW technique as implemented in the Vienna Ab initio Simulation Package (VASP) [27]. The exchange and correlation potential was described using the generalized gradient approximation (GGA) in the Perdew, Burke, and Ernzerhof (PBE) parametrization [9], the Tran-Blaha modified

Becke-Johnson (TB-mBJ) potential [20] and the GW method. The TB-mBJ potential is a modified version of the Becke-Johnson potential [28] used to improve band gaps obtained by the conventional DFT-based methods. The TB-mBJ potential can be written as

$$v_{x,\sigma}^{TB-mBJ}(\mathbf{r}) = cv_{x,\sigma}^{BR}(\mathbf{r}) + (3c - 2)\frac{1}{\pi}\sqrt{\frac{5}{6}}\sqrt{\frac{\tau_{\sigma}(\mathbf{r})}{\rho_{\sigma}(\mathbf{r})}} \quad (1)$$

where  $\rho_{\sigma} = \sum_{i=1}^{N_{\sigma}} |\psi_{i,\sigma}|^2$  is the electron density,  $\tau_{\sigma} = \frac{1}{2} \sum_{i=1}^{N_{\sigma}} \nabla\psi_{i,\sigma}^* \cdot \nabla\psi_{i,\sigma}$  is the kinetic-energy and  $v_{x,\sigma}^{BR}$  is the Becke and Roussel potential [28]. The  $c$  parameter value showed in Eq. 1 is computed with as

$$c = \alpha + \beta \left( \frac{1}{V_{cell}} \int_{cell} \frac{|\nabla\rho_{\sigma}(r')|}{\rho_{\sigma}(r')} d^3r' \right)^{\frac{1}{2}} \quad (2)$$

where  $V_{cell}$  means the unit cell volume,  $\alpha = -0.012$  and  $\beta = 1.023 \text{ bohr}^{\frac{1}{2}}$  are parameters fitted according to experimental values for several materials [20]. It is important to mention that TB-mBJ is a potential-only functional which means there is no corresponding TB-mBJ exchange-correlation energy. This fact, therefore, leads to the impossibility of using TB-mBJ to compute Hellmann-Feynman forces and to compare total energies. The PAW potentials with the valence states  $2s$  and  $2p$  for O atom and  $3d$  and  $4s$  for Zn atom and a basis set up to a kinetic energy cutoff of 450 eV have been used. Integration over the Brillouin zone was performed using a  $9 \times 9 \times 7$  Monkhorst-Pack  $\mathbf{k}$ -points grid. In the optical properties calculations, however, the irreducible Brillouin zone (IBZ) has been sampled with about 500  $\mathbf{k}$ -points. All the calculations have been carried out until the Hellmann-Feynman forces become smaller than  $10^{-3} \text{ eV/\AA}$  and the total energies converged to below  $10^{-4} \text{ eV}$  with respect to the Brillouin zone integration.

As a matter of comparison we have also performed calculations for the dielectric function in the GW approximation. Several approximations lead to different results, such as number of bands the exchange-correlation potential for the starting wave function as well as the use of approximate models for the screening, like plasmon pole approximations. Depending on the starting functional and the details of the calculation, values between 2.1 and 3.6 eV are obtained for  $G_0W_0$  [7, 15, 17, 18, 29, 30], between 2.543.6 for  $GW_0$  [7, 15, 17, 18, 29, 30] and between 3.24.3 for GW [7, 31]. For the  $GW_0$  calculations, a cutoff of 100 eV for the

response functions, as well as 1024 bands have been employed. We obtained 3.2 eV in fair agreement with optical experiments[8] and other calculations within the same approach. [7, 15, 17, 18, 29, 30]. The position of the Zn-3d states has also been corrected to -7.0 eV, closer to the experimental values [15] and in agreement with previous  $\text{GW}_0$  calculations [15, 17].

### III. ELECTRONIC PROPERTIES

ZnO has a wurtzite hexagonal crystal structure that belongs to the  $P6_3mc$  space group with the unit cell containing two Zn cations and two O anions. The lattice parameters are the second nearest neighbor distances and each Zn atom is coordinated by four O atoms which are located at the corners of a slightly distorted tetrahedron. The Zn-O distance along the  $c$  axis is about 1.90 Å which is a little shorter than 1.98 Å of its counterpart perpendicular to the  $c$  axis.

To investigate the optoelectronic properties of ZnO, we firstly calculated the optimized crystal structure of ZnO using the GGA-PBE functional. Thereafter we computed the electronic structure and dielectric functions of ZnO with both GGA-PBE functional and TB-mBJ potential. We found that the GGA-PBE optimized lattice constants for ZnO crystal are  $a = 3.291$  Å and  $c = 5.266$  Å which are in agreement with the experimental values of  $a = 3.250$  Å and  $c = 5.207$  Å[32].

The electronic structure of the ZnO has been calculated with GGA-PBE functional and TB-mBJ potential and they are shown in Fig.1, respectively. The Fermi-level (dotted line) has been specified to be zero in this paper. The upper panel of Fig.1 presents the results for DOS and band structure of ZnO using GGA-PBE functional while the lower panel those calculated with TB-mBJ potential. The DOS spectrum (Fig.1 (a)) possesses three major features in the valence band. The lowest part of it from -18 to -16.8 eV is mainly contributed by O 2s states. The second subband in the energy range between -6 and -4 eV comes mostly from contributions of Zn 3d states whereas the upmost valence subband located between -4 and 0 eV is mainly from O 2p states. We note that there is also orbital hybridization between Zn 3d and O 2p states from -6 to 0 eV. The conduction band originates mainly by the Zn 4s states and the O 2p states. Moreover, the valence and conduction bands are separated by the energy band gap which in our GGA-PBE calculations yields a value of 0.83 eV and this result is consistent with previous calculations [4, 6].

It is known that DFT calculations using standard functionals give a very small band gap as compared with experimental values. This effect in ZnO is further enhanced due to the underestimation of the repulsion between the Zn  $3d$  states and the conduction band [6], which induces to a significant hybridization of the O  $2p$  and Zn  $3d$  levels. In this case, the resulting overly large level of repulsion between the Zn  $3d$  states and valence bands pushes the valence band maximum up.

In order to overcome the band gap problem and have a good description of the electronic structure of ZnO, we applied the TB-mBJ potential on top of the GGA-PBE calculations. We found that the calculated DOS with TB-mBJ method possesses approximately similar features to those of pure ZnO with functional GGA-PBE. However in the TB-mBJ DOS (Fig.1(c)) there is a shift of O  $2s$  states towards lower energy and we note that TB-mBJ potential gives an experimental value

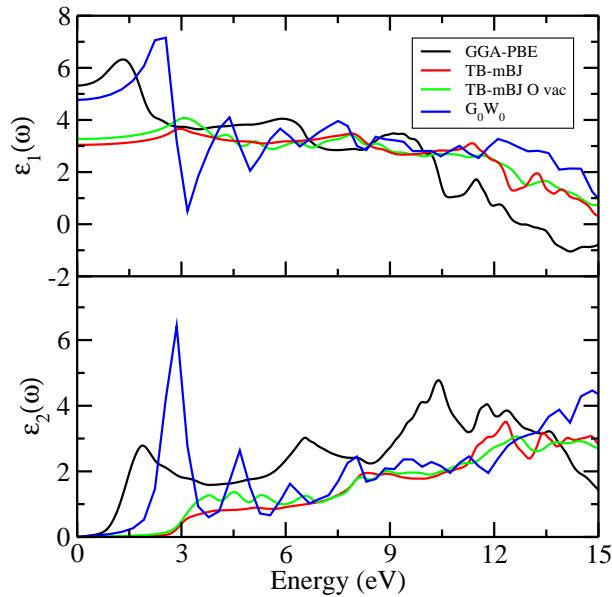


FIG. 2. Average of real (upper panel) and imaginary (lower panel) parts of the dielectric function of ZnO bulk crystal calculated using the GGA-PBE (black line) and TB-mBJ (red line) exchange-correlation functionals and using  $G_0W_0$  method (blue line). Results of the dielectric functions for ZnO with a neutral oxygen vacancy obtained using TB-mBJ (green line) method are also presented.

The band structure along high symmetry lines in the hexagonal Brillouin zone (BZ) using GGA-PBE functional is shown in Fig.1(b). It is evident from the figure that ZnO exhibits a direct band gap with both valence band maximum and conduction band minimum located

at BZ center at  $\Gamma$  point. The lowest two bands (occurring around -16.6 eV) correspond to O  $2s$  levels. The next set of ten bands (occurring around -6 eV) are due to Zn  $3d$  levels. Then six bands from -6 to 0 eV correspond to O  $2p$  bonding states. The first two conduction bands are predominantly formed by Zn  $4s$  states. In Fig.1(d), we present the band structure of ZnO calculated with TB-mBJ potential. We observe a band narrowing in the upper valence band of about 1 eV leading to more localized electrons in the energy range of -6 to 0 eV when compared to GGA-PBE band structure (Fig.1(b)). Additionally, as mentioned before, we obtained a band gap of 3.10 eV with TB-mBJ potential which is much improved relative to the GGA-PBE functional and is in good agreement with the experimental value [8].

#### IV. OPTICAL PROPERTIES

The optical properties of ZnO have been investigated through the imaginary and real parts of the dielectric function. The imaginary part of the dielectric function is calculated directly from the electronic structure through the joint density of states and the matrix elements of the momentum,  $\mathbf{p}$ , between occupied and unoccupied eigenstates according to:

$$\begin{aligned} \epsilon_2^{ij}(\omega) = & \frac{4\pi^2 e^2}{\Omega m^2 \omega^2} \sum_{\mathbf{k}n n'} \langle \mathbf{k}n | p_i | \mathbf{k}n' \rangle \langle \mathbf{k}n' | p_j | \mathbf{k}n \rangle \times \\ & \times f_{\mathbf{k}n} (1 - f_{\mathbf{k}n'}) \delta(E_{\mathbf{k}n'} - E_{\mathbf{k}n} - \hbar\omega). \end{aligned} \quad (3)$$

In this equation,  $e$  is the electron charge,  $m$  the electron mass,  $\Omega$  is the volume of the crystal,  $f_{\mathbf{k}n}$  is the Fermi distribution function and  $|\mathbf{k}n\rangle$  is the crystal wave function corresponding to the  $n^{\text{th}}$  eigenvalue  $E_{\mathbf{k}n}$  with crystal wave vector  $\mathbf{k}$ . The real part of the dielectric function is calculated from  $\epsilon_2$  via the Kramers-Kronig transformation

$$\epsilon_1(\omega) = 1 + \frac{2}{\pi} \int_0^\infty d\omega' \epsilon_2(\omega') \left( \frac{\omega'}{\omega'^2 - \omega^2} \right), \quad (4)$$

where the integral is evaluated setting the frequency cut-off to be several times larger than the frequency range in order to produce accurate results.

In anisotropic materials, dielectric properties must be described by the dielectric tensor. In the case of ZnO, the tensor components can be reduced to only two independent components  $\epsilon_{xx} = \epsilon_{yy} \neq \epsilon_{zz}$ . For materials with weak anisotropy, it has been shown [?] that the dielectric function can be replaced by an average  $\epsilon = \frac{2\epsilon_{xx} + \epsilon_{zz}}{3}$ .

In Fig. 2 we show the average of the parallel and perpendicular directions of light polarization for  $\epsilon_1(\omega)$  and  $\epsilon_2(\omega)$  of ZnO using GGA-PBE (black line), TB-mBJ (red line) and  $G_0W_0$  (blue line) methods. We also show the average of the dielectric function of ZnO with a neutral oxygen vacancy calculated using the TB-mBJ (green line) method. It is worth to mention that  $\epsilon_2(\omega)$  correspond to the experimental light absorption such as observed in electron-energy loss spectroscopy (EELS) [33]. GGA-PBE leads to a too small absorption edge when compared to experimental results [19, 34]. We performed calculations applying the TB-mBJ potential as shown in the red curve. The use of TB-mBJ correction gives a violet shift to the optical band gap of ZnO and it nicely reproduces the experimental [19, 34] absorption edge of ZnO at low computational cost.

The  $\epsilon_2(\omega)$  spectrum of ZnO shows a strong optical anisotropy and it can be roughly divided into three main regions, namely, the low-energy which is the region below 5 eV, the middle-energy one from 5 to 10 eV and the high-energy region above 10 eV. For GGA-PBE calculations, the first peak of  $\epsilon_2(\omega)$  is located at about 2 eV but it appears as a shoulder at about 3 eV for TB-mBJ results. These features are formed mainly due to electronic transitions at the  $\Gamma$  point occurring between O  $2p$  and Zn  $4s$  orbitals. In the middle energy region, there is one peak located at 6.6 eV for the GGA-PBE and it appears less prominent at 8.2 eV for the TB-mBJ. These peaks in the middle-energy region are mainly derived from the transition at M and L points between the Zn  $3d$  and O  $2p$  orbitals. The high-energy region exhibits two principal peaks, around 10 eV and 12 eV for the GGA-PBE, and 12.3 eV and 14.5 eV for the TB-mBJ. The peaks correspond mainly to the transitions from Zn  $3d$  and O  $2s$  orbitals. The TB-mBJ calculations for  $\epsilon_2$  show a good overall agreement with the experimental results, but still fails compared to  $G_0W_0$  calculations. The strong absorption peak around xx eV is very broad with TB-mBJ, which is probably due to the wrong description of the charge density.

The  $GW_0$  shown in blue gives a different picture, with a strong absorption at 3.15 eV. The results for the real part,  $\epsilon_1(\omega)$ , of the dielectric function are consistent with the GGA-PBE and TB-mBJ calculations of  $\epsilon_2(\omega)$ . By looking at the upper panel of Fig.2, it is possible to verify that the optical response of ZnO in the transparent region for GGA-PBE is narrowed compared to the TB-mBJ results due to the shortness of the band gap as previously discussed.



## V. CONCLUSION

In this paper we have investigated the electronic and optical properties of zinc oxide by using density function theory including semilocal exchange-correlation potentials and the  $\text{GW}_0$  method. We found that the band gap and absorption edge of ZnO are in good agreement with experimental data. However, the intensity of the peaks does not agree well with  $\text{GW}_0$  due to the lack of a better description of screening effects. The inclusion of screening effects are primordial to achieve a better agreement with experimental results. Still, the present results strongly support the conclusion that TB-mBJ potential greatly improves the band gaps and electronic structure of simple semiconductors and insulators.

## VI. ACKNOWLEDGEMENT

We are thankful for the financial support from the Brazilian agencies CNPq, CAPES, and FAPESB. A.L.R would like to thank German Science Foundation (DFG) under the program FOR1616.

- 
- [1] Zinc Oxide: Fundamentals, Materials and Device Technology, (Wiley-VC Berlin, 2009).
  - [2] A. Janotti and C. Van de Walle, *Phys. Rev. B* **76**(Oct), 165202 (2007).
  - [3] S. Lany and A. Zunger, *Phys. Rev. B* **81**(Mar), 113201 (2010).
  - [4] S. Lany and A. Zunger, *Phys. Rev. B* **78**(Dec), 235104 (2008).
  - [5] S. Lany and A. Zunger, *Modelling and Simulation in Materials Science and Engineering* **17**(8), 084002 (2009).
  - [6] A. Janotti and C. G. V. de Walle, *Reports on Progress in Physics* **72**(12), 126501 (2009).
  - [7] I. A. Sarsari, C. D. Pemmaraju, H. Salamati, and S. Sanvito, *Phys. Rev. B* **87**(Jun), 245118 (2013).
  - [8] O. Madelung (ed.), *Semiconductors – Basic Data*, 2nd edition edition (Springer, 1996).
  - [9] J. P. Perdew, K. Burke, and M. Ernzerhof, *Phys. Rev. Lett.* **77**(Oct), 3865–3868 (1996).
  - [10] A. V. Krukau, O. A. Vydrov, A. F. Izmaylov, and G. E. Scuseria, *The Journal of Chemical Physics* (2006).
  - [11] C. Adamo and V. Barone, *The Journal of Chemical Physics* **110**, 6158 (1999).

- [12] G. Baym and L. Kadanoff, Phys. Rev. **124**, 287 (1961).
- [13] G. Baym, Phys. Rev. **127**, 1391 (1962).
- [14] L. Hedin, Phys. Rev. **139**, A796 (1965).
- [15] M. Shishkin, M. Marsman, and G. Kresse, Phys. Rev. Lett. **99**(Dec), 246403 (2007).
- [16] P. Rinke, A. Qteish, J. Neugebauer, C. Freysoldt, and M. Scheffler, New Journal of Physics **7**, 126 (2005).
- [17] F. Hüser, T. Olsen, and K. S. Thygesen, Phys. Rev. B **87**, 235 (2013).
- [18] A. Malashevich, M. Jain, and S. Louie, Phys. Rev. B **89**, 075205 (2014).
- [19] P. Gori, M. Rakel, C. Cobet, W. Richter, N. Esser, A. Hoffmann, R. D. Sole, A. Cricenti, and O. Pulci, Phys. Rev. B **81**, 125207 (2010).
- [20] F. Tran and P. Blaha, Phys. Rev. Lett. **102**, 226401 (2009).
- [21] R. B. Araujo, J. S. de Almeida, and A. F. da Silva, J. Appl. Phys. **114**, 183702 (2013).
- [22] D. P. Rai, M. P. Ghimire, and R. K. Thap, Semiconductor **48**, 1411 (2014).
- [23] F. Tran, P. Blaha, and K. Schwarz, J. Phys. Condens. Matter **19**, 196208 (2007).
- [24] B. U. Haq, R. Ahmed, S. Goumri-Said, A. Shaari, and A. Afaq, Phase Transitions **86**, 1167 (2013).
- [25] H. Dixit, R. Saniz, S. Cottenier, D. Lamoen, and B. Partoens, J. Phys. Condens. Matter **24**, 205503 (2012).
- [26] P. E. Blöchl, Phys. Rev. B **50**(Dec), 17953–17979 (1994).
- [27] G. Kresse and D. Joubert, Phys. Rev. B **59**(Jan), 1758–1775 (1999).
- [28] A. D. Becke and E. R. Johnson, J. Chem. Phys. **124**, 221101 (2006).
- [29] C. Friedrich, M. C. Müller, and S. Blügel, Phys. Rev. B **83**(Feb), 081101 (2011).
- [30] B. C. Shih, Y. Xue, P. Zhang, M. L. Cohen, and S. G. Louie, Phys. Rev. Lett. **105**(Sep), 146401 (2010).
- [31] M. Usuda, N. Hamada, T. Kotani, and M. van Schilfgaarde, Phys. Rev. B **66**, 125101 (2002).
- [32] E. H. Kisi and M. M. Elcombe, Acta Cryst. C **45**, 1867 (1989).
- [33] H. J. Morales-Rodriguez and F. M. na, Micron **43**, 177 (2011).
- [34] J. G. E. Jellison and L. A. Boatner, Phys. Rev. B **58**, 3586 (1998).